NRL Report 6971

Laser Radar Range Equation Considerations

P. W. WYMAN

Target Characteristics Branch
Radar Division

December 11, 1969

NAVAL RESEARCH LABORATORY
Washington, D.C.

This document has been approved for public release and sale, its distribution is unlimited

CONTENTS

Abstract ii
Problem Status ii
Authorization ii
Symbols iii

INTRODUCTION 1

DERIVATION OF A GENERALIZED LASER RADAR RANGE EQUATION 1

THE TRANSITION REGION AND $\bar{\gamma}$ 4

Introduction 4
Entrance into the $1/R^4$ Region 7
Entrance into the $1/R^2$ Region 9
Parametric Behavior and Examples 10

EXAMINATION OF $\bar{P}_r$ VS R 13

CONCLUSION 18

ACKNOWLEDGMENT 18

REFERENCES 19

APPENDIX A — Comments on the $1/R^4$ Range Equation 20

APPENDIX B — Comments on the $1/R^2$ Range Equation 21

APPENDIX C — Range Equations when the Received Beam is Smaller than the Receiver 22

APPENDIX D — Reflective Properties of a Surface 23

APPENDIX E — One-Way Atmospheric Transmission Loss τ 26

APPENDIX F — Special Section of the Transition Region when $F \neq 1$ 30

ABSTRACT

Starting with basic physical and beam-target-geometry concepts, a generalized laser radar range equation is derived which holds for a target at any range R in the far field. The equation takes the form $\bar{P}_r \propto \bar{\gamma}/R^2$, where $\bar{P}_r$ is the mean value of the received power and $\bar{\gamma}$ is the mean value of the fraction of the laser beam hitting the target.

By examining the equations for $\bar{\gamma}$, other equations are found for the boundaries of the three radar regions — the $1/R^2$ region, the transition region, and the $1/R^4$ region. These boundaries, and $\bar{\gamma}$ itself, are functions of the spatial jitter of the beam and the degree to which the shape of the beam and the shape of the target geometry are not the same. In the transition region when the jitter is negligible, $\bar{\gamma}$ can be found by inspection (as can be done in the $1/R^2$ and $1/R^4$ regions whether or not the jitter is negligible); the resultant received power then varies as $1/R^3$. In the transition region when the jitter is not negligible, $\bar{\gamma}$ must be calculated from equations before $\bar{P}_r$ can be calculated. For completeness, the reflective properties of a target, its cross section, and the one-way atmospheric transmission loss are examined. The relationships derived in this report are general in that they are valid at any (e.g., microwave) wavelengths.

PROBLEM STATUS

This is a final report on one phase of the problem; work on other phases continues.

AUTHORIZATION

NRL Problems R02-24A, R05-29, and R06-38
Projects AO-535-208/652-1/F099-05-02
and RF-17-344-401-4509

Manuscript submitted August 6, 1969.

SYMBOLS

A_B area of beam (m^2), $= \Omega_t R^2 = L_{Bx} L_{Bz}$

A_i irradiated target area normal to the beam (m^2)

A_r receiver area (m^2)

A_T area of the target (m^2)

F shape factor $= (L_{Tx}/L_{Tz})/(\theta_x/\theta_z)$

h_T target height (m)

H_i incident irradiance (W/m^2)

J intensity (W/sr); with subscripts r and t, refers to reflected and transmitted intensity, respectively

k relative beam stability in the x direction, $= \theta_x/\Delta_x$

k' relative beam stability in the z direction, $= \theta_z/\Delta_z$

L_{Tx} target dimension parallel to x direction (m), $= w_T \cos\omega$

L_{Tz} target dimension parallel to z direction (m), $= h_T \cos\eta$

L_{Bx} beam dimension parallel to x direction (m), $= \theta_x R$

L_{Bz} beam dimension parallel to z direction (m), $= \theta_z R$

N_r reflected radiance ($W/sr\text{-}m^2$)

P_r received power (W)

p_t transmitted power (W)

R range to target (m)

V horizontal visibility range (m)

w_T target width (m)

x, z Cartesian coordinates subscripts

α azimuth angle (measured in the plane of the surface)

$\beta(h)$ atmospheric attenuation coefficient at a height h (m^{-1})

γ_x fraction of the beam on the target in the x direction

γ_z fraction of the beam on the target in the z direction

γ fraction of the total beam hitting the target, $= A_i/A_B = \gamma_x \gamma_z$

Δ_x angular beam jitter in the x direction (radians)

Δ'_x linear beam jitter in the x direction (m), $= \Delta'_x R$

η orientation of target relative to z direction

θ_x beam divergence in the x direction (radians)

θ_z beam divergence in the z direction (radians)

ρ' bidirectional reflectance-distribution function (sr^{-1})

ρ_d bidirectional reflectance, $= \int_h \rho' \sin\psi_r \cos\psi_r \, d\psi_r d\alpha_r$

σ^0 radar cross section/unit area

σ radar cross section (m^2)

τ one-way atmospheric transmission loss, $= e^{-\beta R}$ when β is constant

ψ elevation angle (measured from the normal to the surface)

ω orientation of target relative to x direction

Ω_t transmitter solid angle (sr), $= \theta_x \theta_z$

LASER RADAR RANGE EQUATION CONSIDERATIONS

INTRODUCTION

In the field of microwave radars, a target at any range R is almost always either much larger or much smaller than the radar beam, and thus the mean value of the receiver power $\bar{P}_r$ either varies as $1/R^2$ or $1/R^4$, respectively. However, with narrow-beamwidth laser radars the radar beam may also be about the same size as the target. Thus, with laser radars there are three possible regions — a $1/R^2$ region, a transition region (TR), and a $1/R^4$ region. The purpose of this report is to derive a generalized laser radar range equation which is valid for all three regions, to find equations for calculating the boundaries of the TR, and to determine how the TR varies with various parameters. The parameters of the generalized range equation will also be examined.

In this analysis the following is assumed: the radar system is monostatic; the beam has a rectangular cross section with no side lobes) and a uniform irradiance H_i at the target; and the target is flat and rectangular, with uniform reflective properties across its surface.* In addition, the target can be tilted at any angle to the beam.

In Appendices A and B some comments are made about the $1/R^2$ and $1/R^4$ laws. Appendix C gives the derivation of various range equations for the special case of the received beam being smaller than the receiver. The parameters describing the reflective properties of a surface are defined and discussed in Appendix D. There are derivations in Appendix E of equations for the one-way transmission loss due to the atmosphere. Appendix F has a discussion of a special portion of the TR.

DERIVATION OF A GENERALIZED LASER RADAR RANGE EQUATION

In Ref. 1 a new radar range equation parameter, $\bar{\gamma}$, was first introduced. Defined as the mean value (over many pulses) of the fraction of the beam hitting the target, this parameter will allow the derivation of a generalized laser radar range equation. From Fig. 1 it is seen that, for any given pulse, the fraction γ of the beam hitting the target is given by $\gamma = A_i/A_B$, where A_i is the portion of the beam hitting the target (on any given pulse) and A_B is the cross-sectional area of the laser beam. In the following it will be assumed that the target is in the far field of the transmitter and that the receiver is in the far field of the target.

The reflected intensity J_r (in W/sr) is related to the incident irradiance H_i (in W/m^2) by just a constant C, so that

$$J_r = C H_i \ . \tag{1}$$

*The results obtained, based on these assumptions, can be extended to nonrectangular target and beam shapes as long as the shapes are approximated by rectangles.

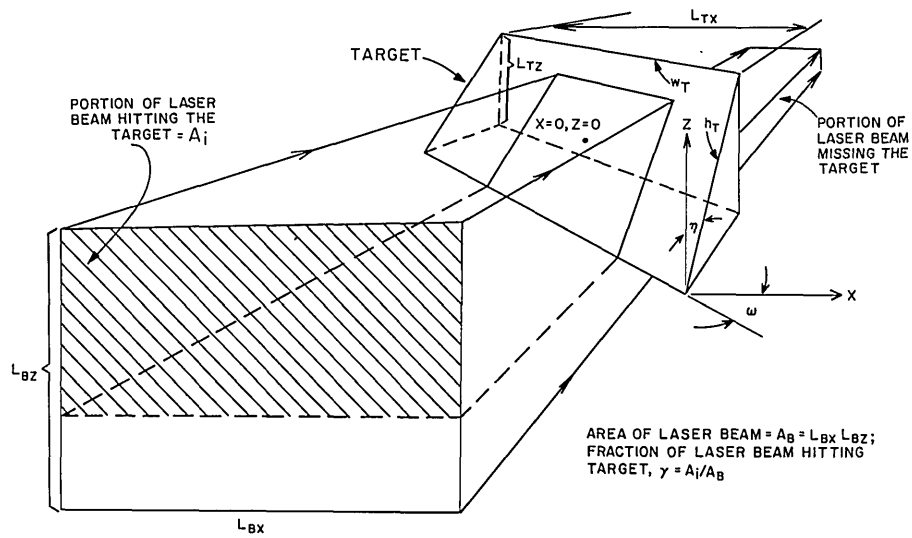

Fig. 1 - Laser radar beam-target geometry

Since

$$H_i = \tau J_t / R^2 \tag{2}$$

and

$$P_r = \tau J_r A_r / R^2 \ , \tag{3}$$

the received power is given by

$$P_r \text{ (watts)} = \tau^2 C J_t A_r / R^4 \tag{4}$$

where

τ = one-way atmospheric transmission loss,

J_t = transmitter intensity (W/sr),

R = target range (m), and

A_r = receiver area (m^2).

It should be noted that Eq. (3) holds only when the area of the reflected beam at the receiver is greater than the area of the receiver itself. This is generally the case. (See Appendix C when this is not the case.)

The parameter C will now be examined by examining J_r. Nicodemus (2-4) defines the bidirectional reflectance-distribution function ρ' at a point as

$$\rho'(\psi_i, \alpha_i : \psi_r, \alpha_r) = \frac{dN_r}{dH_i} \tag{5}$$

where

ψ = elevation angle (measured from the normal to the surface),

α = azimuth angle (measured in the plane of the surface),

i and r = incident and reflected, respectively, and

N_r = reflected radiance (in W/m^2-sr) in the direction of the radar.

(For notational convenience, $\rho'(\psi_i, \alpha_i : \psi_r, \alpha_r)$ will be shortened to just ρ'.) Generally ρ' is independent of H_i and, therefore,

$$\rho'(\text{in sr}^{-1}) = N_r/H_i \ . \tag{6}$$

Assuming that ρ' and H_i are constant over the surface of the target yields

$$\rho' H_i A_i = \int_{A_i} N_r \, dA \tag{7}$$

where A_i is the irradiated area of the target normal to the beam (see Fig. 1); A_i can also be defined as the portion of the beam hitting the target (on any given pulse). Since the integral of N_r over A_i is by definition (2) equal to J_r, Eq. (7) becomes

$$J_r = \rho' H_i A_i \ . \tag{8}$$

Combining Eqs. (1) and (8) yields

$$\rho' A_i = C \ , \tag{9}$$

and substituting this into Eq. (4) yields

$$P_r = \tau^2 \rho' A_i J_t A_r / R^4 \ . \tag{10}$$

Since

$$\gamma = A_i / A_B \tag{11}$$

and

$$\begin{aligned} A_B &= \Omega_t R^2 \ , \\ A_i &= \gamma \Omega_t R^2 \end{aligned} \tag{12}$$

where Ω_t is the solid angle of beam divergence. Using Eq. (12) and the fact that the power of the transmitter is

$$P_t = J_t \Omega_t \ ,$$

Eq. (10) becomes

$$P_r = P_t \tau^2 \rho' \gamma A_r / R^2 \ . \tag{13}$$

Since γ is a function not only of the geometry shown in Fig. 1 but also of the spatial jitter of the beam, it must be handled on a statistical basis by considering its mean value $\bar{\gamma}$. If it is assumed that all of the other parameters in Eq. (13) are constant, then the equation for the mean value of the received power (over many pulses) becomes

$$\bar{P}_r = P_t \tau^2 \rho' \bar{\gamma} A_r / R^2 \ . \tag{14}$$

This is the *generalized laser radar range equation*.

The relationship between C and the radar parameter of target cross section σ will now be determined. In the field of microwave radars the standard target is taken to be an isotropically reflecting sphere. This standard results (5) in the following definition of σ:

$$\sigma \equiv 4\pi J_r / H_i \tag{15}$$

and thus, $\sigma = 4\pi C$. In the optical radar field the standard target is sometimes taken to be a diffuse flat surface, and this standard results (6) in the following definition of σ:

$$\sigma = \pi J_r / H_i \tag{16}$$

and thus $\sigma = \pi C$. From now on in this report, however, just the microwave concepts and definitions, based on an isotropic standard, will be used.

Combining Eqs. (8) and (15) yields

$$\sigma = 4\pi \rho' A_i \ . \tag{17}$$

Another parameter introduced (7) in the radar field is σ^0, the radar cross section per unit area, and it is equal to σ divided by the irradiated target area normal to the beam, i.e.,

$$\sigma = \sigma^0 A_i \ . \tag{18}$$

Combining Eqs. (17) and (18) yields

$$\sigma^0 = 4\pi \rho' \ . \tag{19}$$

When Eq. (19) is substituted into Eq. (14), the range equation becomes

$$\bar{P}_r = P_t \tau^2 \sigma^0 \bar{\gamma} A_r / (4\pi R^2) \ . \tag{20}$$

In Appendix A the familiar $1/R^4$ microwave radar range equation is derived from Eq. (20). It should be noted that Eqs. (14) and (20) hold for targets at any range.

THE TRANSITION REGION AND $\bar{\gamma}$

Introduction

Two things cause the existence of a transition region (TR): spatial jitter of the laser beam, and the geometrical relationship between the target and the beam. An example of a system operating in the TR is seen in Fig. 2 where, even when there is no jitter, operation is in neither the $1/R^4$ nor the $1/R^2$ region. This is true since in the x direction the beam is larger than the target, while in the z direction the beam is smaller than the target.

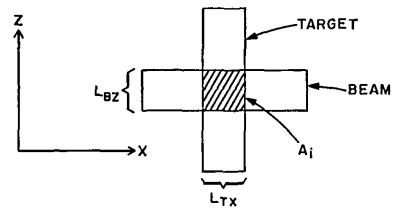

Fig. 2 - Simplified laser radar beam-target geometry

Where the TR begins and ends will now be determined by examining the equations from Ref. 1 for $\bar{\gamma}_x$ and $\bar{\gamma}_z$, the mean values of the fractions of the beam on target in the x and z directions, respectively. The product of $\bar{\gamma}_x$ and $\bar{\gamma}_x$ is equal to γ (if γ_x and γ_z are, as has been assumed statistically independent). The following equations are for the x direction, but identical equations hold for the z direction.*

When the beam is greater than the target (i.e., when $L_{Bx} \geq L_{Tx}$),

$$\bar{\gamma}_x = \frac{2}{L_{Bx}} \left[L_{Tx} \int_0^{y_1} \frac{\exp(-y^2/2)\, dy}{\sqrt{2\pi}} + \left(\frac{L_{Bx} + L_{Tx}}{2} \right) \int_{y_1}^{y_2} \frac{\exp(-y^2/2)\, dy}{\sqrt{2\pi}} + \frac{\Delta_x'}{\sqrt{2\pi}} \exp(-y^2/2) \Bigg|_{y_1}^{y_2} \right]. \tag{21}$$

When the beam is smaller than the target (i.e., when $L_{Bx} \leq L_{Tx}$),

$$\bar{\gamma}_x = \frac{2}{L_{Bx}} \left[L_{Bx} \int_0^{y_3} \frac{\exp(-y^2/2)\, dy}{\sqrt{2\pi}} + \left(\frac{L_{Bx} + L_{Tx}}{2} \right) \int_{y_3}^{y_2} \frac{\exp(-y^2/2)\, dy}{\sqrt{2\pi}} + \frac{\Delta_x'}{\sqrt{2\pi}} \exp(-y^2/2) \Bigg|_{y_3}^{y_2} \right]. \tag{22}$$

In Eqs. (21) and (22)

$L_{Tx} = w_T \cos\omega$ = target size in the x direction (m),

$L_{Bx} = \theta_x R$ = beam size in the x direction (m),

θ_x = beam divergence in the x direction (radians),

$\Delta_x' = \Delta_x R$ = linear beam jitter in the x direction (m),

Δ_x = angular beam jitter in the x direction (radians),

$$y_1 = \frac{L_{Bx} - L_{Tx}}{2\Delta_x'},$$

$$y_2 = \frac{L_{Bx} + L_{Tx}}{2\Delta_x'},$$

*The use of Cartesian coordinates leads quite naturally to the consideration of rectangular-shaped beams and targets. For nonrectangular beams and/or targets, the shapes must be approximated by rectangles in order to use this approach.

and

$$y_3 = \frac{L_{Tx} - L_{Bx}}{2\Delta_x'} .$$

It should be noted for future reference that

$$y_1 + y_2 = L_{Bx}/\Delta_x' = \theta_x/\Delta_x \equiv k = y_2 - y_3$$

Equations (21) and (22) can be simplified if the following notation is used:

$\phi(y) = e^{-y^2/2}/\sqrt{2\pi} =$ normal or Gaussian distribution (with zero mean),

$$G_1 = \int_0^{y_1} \phi(y)\, dy ,$$

$$G_2 = \int_{y_1}^{y_2} \phi(y)\, dy ,$$

$$G_3 = \int_0^{y_3} \phi(y)\, dy ,$$

$$G_4 = \int_{y_3}^{y_2} \phi(y)\, dy ,$$

$$E_1 = \phi(y)\Big|_{y_1}^{y_2} ,$$

and

$$E_2 = \phi(y)\Big|_{y_3}^{y_2} .$$

Therefore when $L_{Bx} \geq L_{Tx}$

$$\bar{\gamma}_x = \frac{2}{L_{Bx}}\left[L_{Tx}G_1 + \left(\frac{L_{Bx} + L_{Tx}}{2}\right)G_2 + \Delta_x' E_1\right] , \tag{23}$$

and when $L_{Bx} \leq L_{Tx}$

$$\bar{\gamma}_x = \frac{2}{L_{Bx}}\left[L_{Bx}G_3 + \left(\frac{L_{Bx} + L_{Tx}}{2}\right)G_4 + \Delta_x' E_2\right] . \tag{24}$$

In examining Eq. (23) it is seen that if the bracketed factor approaches $L_{Tx}/2$, then $\bar{\gamma}_x$ approaches L_{Tx}/L_{Bx}. If the same behavior occurs in the z direction, i.e., if $\bar{\gamma}_z$ approaches L_{Tz}/L_{Bz}, then $\bar{\gamma}$, which equals $\bar{\gamma}_x\bar{\gamma}_z$, will approach $L_{Tx}L_{Tz}/L_{Bx}L_{Bz}$. Since

$\Omega_t = \theta_x \theta_z$, $\bar{\gamma}$ will thus be approximately equal to $L_{Tx} L_{Tz}/\Omega_t R^2$. Substituting this value of $\bar{\gamma}$ into Eq. (14) yields $\bar{P}_r \propto 1/R^4$. Under these conditions the target is said to be in the $1/R^4$ region.

Similarly, in examining Eq. (24) it is seen that if the bracketed factor approaches $L_{Bx}/2$, then $\bar{\gamma}_x$ approaches one. If the same thing happens simultaneously in the z direction, i.e., if $\bar{\gamma}_z \approx 1$, then $\bar{\gamma} \approx 1$, and when $\bar{\gamma} \approx 1$, Eq. (14) yields $\bar{P}_r \propto 1/R^2$. Under these conditions the target is said to be in the $1/R^2$ region.

In general, however, $\bar{P}_r \propto \bar{\gamma}/R^2$, and when the target is in neither the $1/R^4$ nor the $1/R^2$ region, then it is said to be in the transition region. Thus, there are three radar regions: the $1/R^2$ region, then a transition region, and then the $1/R^4$ region.

Entrance Into the $1/R^4$ Region

In order to enter the $1/R^4$ region the bracketed factor in Eq. (23) must approach $L_{Tx}/2$ and simultaneously it must approach $L_{Tz}/2$ when examined in the z direction. Equation (23) can be modified by introducing a parameter k called the relative beam stability in the x direction, which is defined as the ratio in the x direction between the beam size and the spatial jitter. Thus, $k = \theta_x/\Delta_x = L_{Bx}/\Delta_x'$. Similarly $k' = \theta_z/\Delta_z$. Rewriting Eq. (23) using k yields

$$\bar{\gamma}_x = \frac{2L_{Tx}}{L_{Bx}} \left[G_1 + \left(\frac{k - y_1}{k - 2y_1} \right) G_2 + \frac{E_1}{k - 2y_1} \right] . \tag{25}$$

The bracket in Eq. (25) must approach 1/2 if $\bar{\gamma}_x$ is going to approach L_{Tx}/L_{Bx}. Since $y_2 = k - y_1$ (see definition on p. 6), k and y_1 fully determine the value of the bracket. As a first guess, $y_1 = 2$ is chosen, since for this value of y_1, $G_1 \approx 1/2$. The results of the evaluation of the bracket when $y_1 = 2$ are shown in the ϵ_1 curve in Fig. 3. Here the error ϵ_1, which is the difference between the value 1/2 and the value of the bracket in Eq. (25), is plotted as a percentage versus k. For values of $k > 4 = 2y_1$, the percentage error is reasonably low (4% or less). Larger values of y_1 have been used in evaluating the bracket, and as long as $k > 2y_1$, the percentage error stays low. Therefore, when $y_1 \geq 2$ and $k > 2y_1$, $\bar{\gamma}_x \approx L_{Tx}/L_{Bx}$.

The reason why k must be greater than $2y_1$ can be seen from a manipulation of the defining equation of y_1, which yields

$$R = \frac{L_{Tx}}{(k - 2y_1)\Delta_x} . \tag{26}$$

This equation also explains the asymptotic behavior of the ϵ_1 curve at $k = 4$, since for this curve $y_1 = 2$.

The physical basis of why the y_1 inequality (i.e., $y_1 \geq 2$) holds will now be shown. Defining the range R_x at which $y_1 = 2$ yields

$$R_x \equiv \frac{L_{Tx}}{(k - 4)\Delta_x} = \frac{L_{Tx}}{\theta_x - 4\Delta_x} . \tag{27}$$

And so at R_x, $\bar{\gamma}_x \approx L_{Tx}/L_{Bx}$. (It should be noted that at any valid R_x, Eq. (27) shows that k is automatically greater than four.) At ranges beyond R_x, where the target looks more and more like a point to the laser radar, $\bar{\gamma}_x$ approaches closer and closer to L_{Tx}/L_{Bx}.

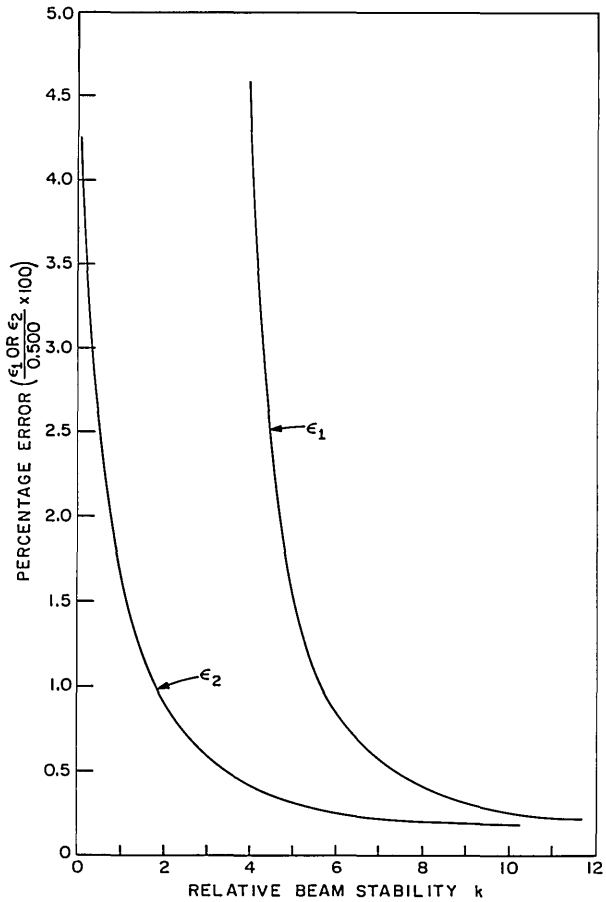

Fig. 3 - Percentage error ϵ vs relative beam stability k. ϵ_1 pertains to $L_{Bx} \geq L_{Tx}$ and ϵ_2 pertains to $L_{Bx} \leq L_{Tx}$ where L_{Bx} and L_{Tx} are the beam and target sizes, respectively, in the x direction.

This line of reasoning leads to the conclusion that when $R \geq R_x$, $\bar{\gamma}_x \approx L_{Tx}/L_{Bx}$; it can also be shown that $R \geq R_x$ yields $y_1 \geq 2$. In summary it is seen that when $y_1 \geq 2$ and $k > 2y_1$, then $\bar{\gamma}_x \approx L_{Tx}/L_{Bx}$.

Exactly the same analysis can be carried out in the z direction, with the result that when

$$R \geq R_z \equiv \frac{L_{Tz}}{\theta_z - 4\Delta_z}, \tag{28}$$

then $\bar{\gamma}_z \approx L_{Tz}/L_{Bz}$. Therefore, when R is greater than both R_x and R_z, $1/R^4$ operation occurs since then $\bar{\gamma}_x \approx L_{Tx}/L_{Bx}$ *and* $\bar{\gamma}_z \approx L_{Tz}/L_{Bz}$.

The physical significance of R being greater than R_x can be seen by manipulating $R \geq L_{Tx}/(\theta_x - 4\Delta_x)$ to give $L_{Bx} \geq L_{Tx} + 4\Delta'_x$.† This inequality in effect states that in the x

†If R_x had been defined at some general value of y_1 greater than 2, say y_1^*, then $R \geq R_x$ would have yielded $L_{Bx} \geq L_{Tx} + 2y_1^*\Delta'_x$.

direction if $R \geq R_x$, then the beam is larger than the target by at least four times the jitter. If this is the case, then the target will be fully illuminated (in the x direction) almost all of the time.

Entrance Into the $1/R^2$ Region

In order to enter into the $1/R^2$ region the bracketed factor in Eq. (24) must approach $L_{Bx}/2$, and simultaneously it must approach $L_{Bz}/2$ when examined in the z direction. Introducing k into Eq. (24) yields

$$\bar{\gamma}_x = 2\left[G_3 + \left(\frac{k + y_3}{k}\right) G_4 + E_2/k\right] . \tag{29}$$

The bracket in Eq. (29) must approach 1/2 if $\bar{\gamma}_x$ is going to approach one. Since $y_2 = k + y_3$, k and y_3 fully determine the value of this bracket. As a first guess, $y_3 = 2$ is chosen since, for this value of y_3, $G_3 \approx 1/2$. The results of evaluating the bracket when $y_3 = 2$ are shown in the ϵ_2 curve in Fig. 3. The error ϵ_2, which is the difference between the value 1/2 and the value of the bracket in Eq. (29), is also plotted as a percentage versus k. For values of $k > 0$, the percentage error is less than 4%. When larger values of y_3 are used in evaluating the bracket, the percentage error still remains low. Therefore, when $y_3 \geq 2$ and $k > 0$, then $\bar{\gamma}_x \approx 1$.

If the defining equation of y_3 is manipulated, it yields

$$R = \frac{L_{Tx}}{(k + 2y_3)\Delta_x} . \tag{30}$$

It is thus seen that k only has to be greater than zero. Since $k = \theta_x/\Delta_x$, if k equaled zero it would mean that the jitter Δ_x was infinite, since the beam size θ_x can't go to zero. Therefore, the asymptotic behavior of ϵ_2 at $k = 0$ is to be expected.

The physical basis of why the y_3 inequality (i.e., $y_3 \geq 2$) is used will now be shown. Defining the range at which $y_3 = 2$ as R'_x yields

$$R'_x = \frac{L_{Tx}}{(k+4)\Delta_x} = \frac{L_{Tx}}{\theta_x + 4\Delta_x} . \tag{31}$$

Therefore, at R'_x, $\bar{\gamma}_x \approx 1$ (since $y_3 = 2$). At ranges shorter than R'_x, as the beam continues to get smaller than the target, the beam misses the target less and less frequently so that $\bar{\gamma}_x$ gets closer and closer to one. Therefore, when $R \leq R'_x$, $\bar{\gamma}_x \approx 1$; it can also be shown that $R \leq R'_x$ yields $y_3 \geq 2$. In summary it is seen that when $y_3 \geq 2$ and $k > 0$, then $\bar{\gamma}_x \approx 1$.

Exactly the same analysis can be carried out in the z direction, with the result that when

$$R \leq R'_z \equiv \frac{L_{Tz}}{\theta_z + 4\Delta_z} , \tag{32}$$

then $\bar{\gamma}_z \approx 1$. Therefore, when R is less than both R'_x and R'_z, $1/R^2$ operation occurs since then $\bar{\gamma}_x \approx 1$ *and* $\bar{\gamma}_z \approx 1$, and thus $\bar{\gamma} \approx 1$.

The physical significance of R being less than or equal to R'_x can be seen by manipulating $R \leq L_{Tx}/(\theta_x + 4\Delta_x)$ to give $L_{Tx} \geq L_{Bx} + 4\Delta'_x$.† This inequality in effect states that in the x direction if $R \leq R'_x$, then the target is larger than the beam by at least four times the jitter. If this is the case, then the beam is almost always entirely on the target in the x direction.

Summarizing then, when $R = R_x$ or R_z, depending on which is greater, the $1/R^4$ region starts, and when $R = R'_x$ or R'_z, depending on which is smaller, then the $1/R^2$ region starts.

Parametric Behavior and Examples

The Effect of the Shape Factor on the TR — In order to study the effect of the situation geometry, by itself, on the TR, the beam jitter will be assumed negligible (i.e., $\Delta_x = \Delta_z \approx 0$) in this section. Equations (27) and (31) thus yield

$$R_x = R'_x = L_{Tx}/\theta_x \quad , \tag{33}$$

and Eqs. (28) and (32) yield

$$R_z = R'_z = L_{Tz}/\theta_z \quad . \tag{34}$$

Thus, the TR extends from R_x to R_z, or vice-versa.

A parameter which describes the geometrical relationship between the target and the beam is now introduced: the shape factor F is defined as

$$F \equiv \frac{L_{Tx}/L_{Tz}}{\theta_x/\theta_z} = \frac{L_{Tx}/\theta_x}{L_{Tz}/\theta_z} = \frac{L_{Tx}/L_{Bx}}{L_{Tz}/L_{Bz}} \, . \tag{35}$$

Thus, F reflects the degree of mismatching between the shape of the target and the shape of the beam.‡ From Eqs. (33) - (35), the shape factor F becomes

$$F = R_x/R_z \quad , \tag{36}$$

and this yields

$$R_z = \frac{L_{Tx}}{F\theta_x} \, . \tag{37}$$

Thus, the TR extends from $R = R_x = L_{Tx}/\theta_x$ to $R = R_z = L_{Tx}/F\theta_x$, or vice-versa. When $F < 1$, $R_z > R_x$, and the TR extends from R_x to R_z. As F approaches one, R_x approaches R_z and the TR shrinks to just a line. As F now increases beyond one, R_x becomes greater than R_z, and the TR then extends from R_z to R_x. The following general figures (Figs. 4(a) - (c)) can now be drawn. Since the non-TR conditions of Fig. 4(b) ($F = 1$ and $\Delta_x = \Delta_z \approx 0$ mrad) don't usually exist, there is thus usually no abrupt change between the $1/R^2$ region and the $1/R^4$ region. Figure 5 shows a typical case when $F = 1/6$. Here $L_{Tx}/L_{Tz} = 1/6$ and $\theta_x/\theta_z = 1/1$, and therefore $F = (1/6)/(1/1) = 1/6$.

---

†If R'_x had been defined at some general value of y_3 greater than 2, say y_3^*, then $R \leq R'_x$ would have yielded $L_{Tx} \geq L_{Bx} + 2y_3^*\Delta'_x$.

‡"Shape" here will also connote the orientations of both the beam and the target.

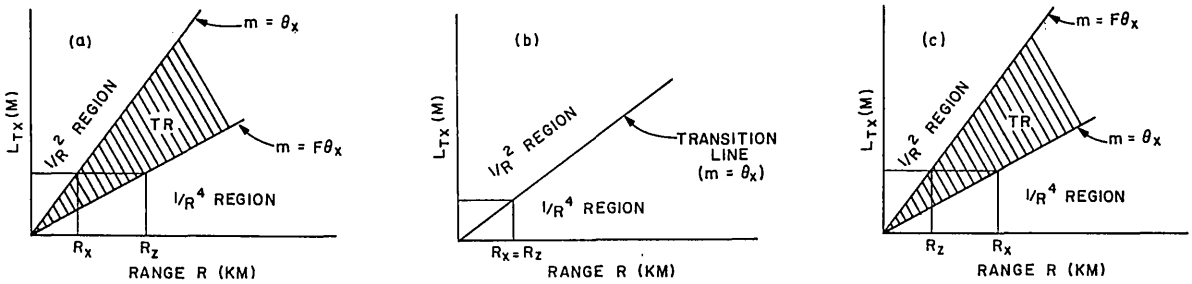

Fig. 4 - Radar regions when $\Delta_x = \Delta_z \approx 0$, and (a) $F < 1$, (b) $F = 1$, and (c) $F > 1$.

Fig. 5 - Geometry when $F = 1/6$

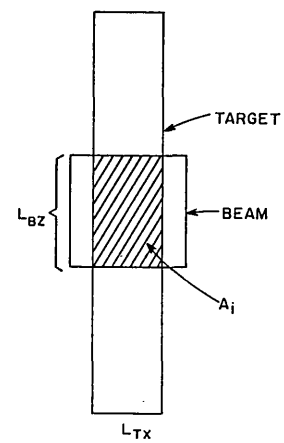

The Effect of Jitter on the TR — In order to study the effect of jitter by itself, the effect of shape has to be negated by making $F = 1$, and this has been done in this section by making

$$L_{Tx}/L_{Tz} = \theta_x/\theta_z = \Delta_x/\Delta_z \tag{38}$$

It can also be shown that when Eq. (38) holds, $R_x = R_z$ and $R'_x = R'_z$, and therefore all the calculations can be carried out in just the x direction.

Figure 6 shows the case of negligible jitter for various values of θ_x, and naturally it is similar to Fig. 4(b) since once again $F = 1$ and $\Delta_x = \Delta_z \approx 0$ mrad. As the jitter becomes significant, the TR comes into being, and Fig. 7 shows how the extent of the TR increases as the jitter increases for any given value of L_{Tx}. If two laser radar systems have the same value of $k (= \theta_x/\Delta_x)$, then that system which has the smaller beam divergence and jitter will be the one whose TR occurs further out in range for any given value of L_{Tx}; this is shown in Fig. 8.

General Example — The effect of shape on the TR has been studied (Fig. 4) by making the shape factor F variable and the jitter constant ($\Delta_x = \Delta_z \approx 0$). Then the reverse was done, i.e., the effect of the jitter on the TR was studied (Fig. 7) by making the jitter variable and the shape factor constant ($F = 1$). And now the combined effects of both shape and jitter will be shown in a typical example. Let the following values be assumed:

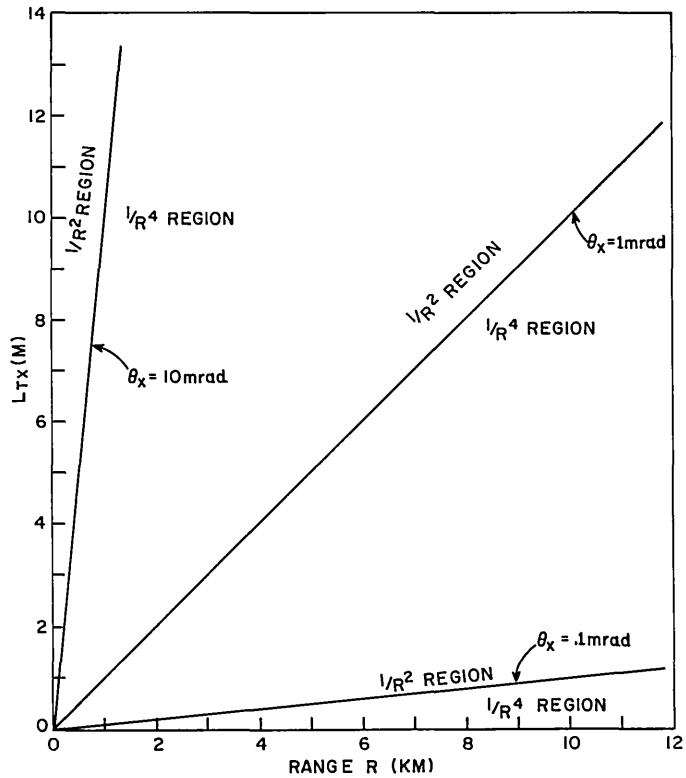

Fig. 6 - Relationship between radar regions and beam divergence θ_x when $F = 1$ and the jitter Δ_x is negligible

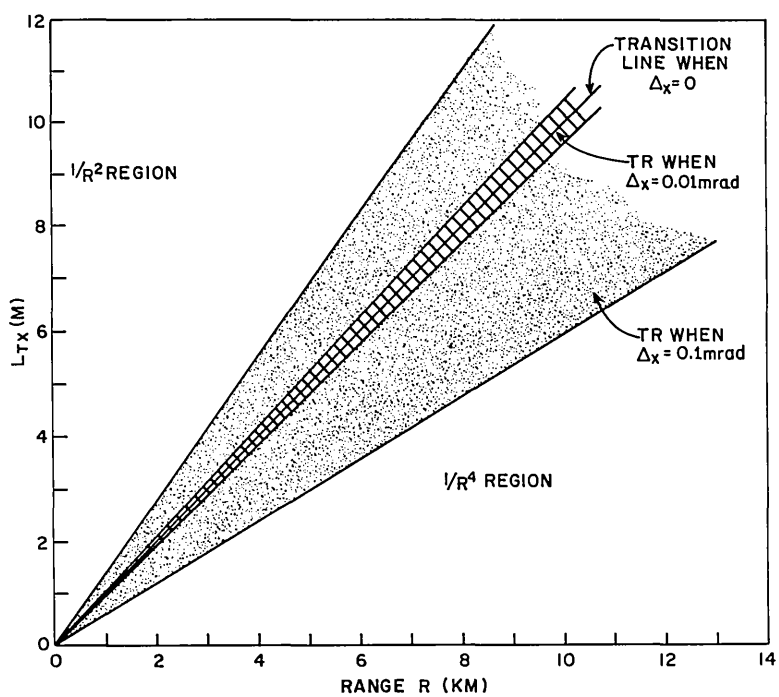

Fig. 7 - Relationship between radar regions and the amount of jitter Δ_x when $F = 1$ and the beam divergence θ_x is constant (θ_x = 1 mrad)

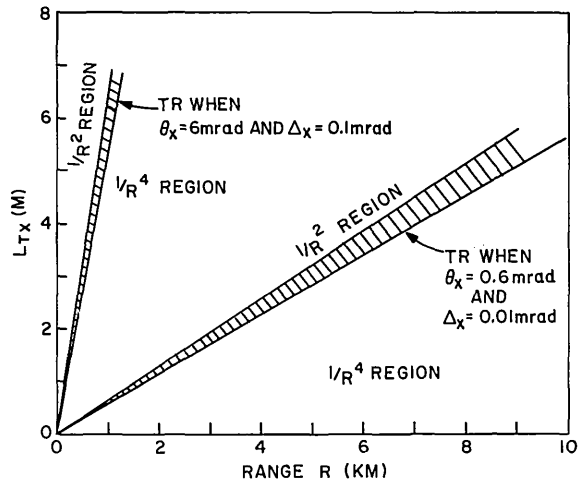

Fig. 8 - Radar regions when $F = 1$ and the relative beam stability k remains constant ($k = 60$)

$$L_{Tx} = 0.5 \text{ m} \qquad L_{Tz} = 3 \text{ m}$$

$$\theta_x = 0.5 \text{ mrad} \qquad \theta_z = 0.5 \text{ mrad}$$

$$\Delta_x = 0.05 \text{ mrad} \qquad \Delta_z = 0.1 \text{ mrad} .$$

Then

$$R_x = \frac{L_{Tx}}{\theta_x - 4\Delta_x} = \frac{0.5 \text{ m}}{0.3 \text{ mrad}} = 1.67 \text{ km} \quad \text{and} \quad R_z = \frac{3 \text{ m}}{0.1 \text{ mrad}} = 30 \text{ km} ,$$

and therefore the $1/R^4$ region starts at 30 km. Also,

$$R'_x = \frac{L_{Tx}}{\theta_x + 4\Delta_x} = \frac{0.5 \text{ m}}{0.7 \text{ mrad}} = 0.7 \text{ km} \quad \text{and} \quad R'_z = \frac{3 \text{ m}}{0.9 \text{ mrad}} = 3.3 \text{ km} .$$

Therefore, the $1/R^2$ region starts at 0.7 km. This example is shown in Fig. 9

EXAMINATION OF $\bar{P}_r$ VS R

Having examined the effects of the shape factor F and jitter Δ_x on the TR, the question now arises as to how they effect $\bar{\gamma}$ and $\bar{P}_r$. Since Eq. (20) states that $\bar{P}_r = M\,\bar{\gamma}/R^2$ (where $M = P_t\,\tau^2\,\sigma^0 A_r/4\pi$), $\bar{\gamma}$ and $\bar{P}_r$ can be easily related if M is a constant. In this section it will be assumed that $\beta = 0$, and therefore $\tau = 1$, and that M is constant.

When the jitter of the beam is negligible, $\bar{\gamma}$ can be found for any F just by inspection. Since $\bar{\gamma}_x$ is defined as the mean value of the beam hitting the target in the x direction, if the beam is smaller than the target in the x direction, $\bar{\gamma}_x = 1$. If the beam is larger than the target in the x direction, $\bar{\gamma}_x = L_{Tx}/L_{Bx} = (L_{Tx}/\theta_x)/R$. Therefore, with no jitter, when the beam is smaller than the target in both directions, $\bar{\gamma} = \bar{\gamma}_x \cdot \bar{\gamma}_z = 1$ and $\bar{P}_r = M/R^2$; when the beam is larger than the target in both directions, $\bar{\gamma} = L_{Tx}L_{Tz}/L_{Bx}L_{Bz} = (L_{Tx}L_{Tz}/\Omega_t)/R^2$ and $\bar{P}_r = (M L_{Tx}L_{Tz}/\Omega_t)/R^4$. These are the basic range relationships in the

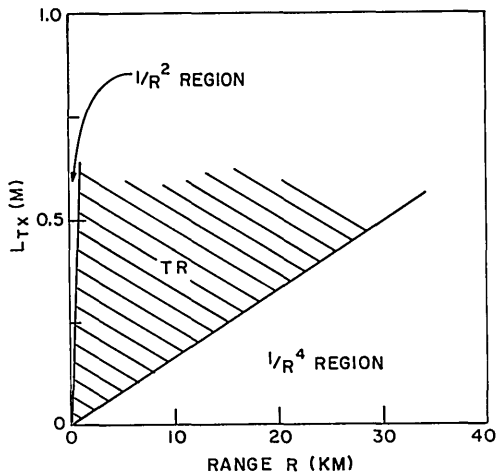

Fig. 9 - General example of radar regions

$1/R^2$ and $1/R^4$ regions when there is no jitter. When $F = 1$ these are the only two possible geometrical situations and the only two range relationships. However, when $F \neq 1$, there is, in addition to the $1/R^2$ and $1/R^4$ regions, a TR in which in one direction the beam can be larger than the target, while in the other direction the beam can be smaller than the target (e.g., see Fig. 2). When this occurs $\bar{\gamma} = (L_{Tx}/\theta_x)/R$ or $(L_{Tz}/\theta_z)/R$, depending on in which direction the beam is greater than the target. Therefore when there is no jitter and the TR is only due to $F \neq 1$, $\bar{P}_r \propto 1/R^3$ (see Figs. 4(a) and (c)). When and where this unique $1/R^3$ region exists has now been determined.

Two other basic cases arise when jitter cannot be neglected, and thus there are four cases altogether. With the introduction of jitter, if the target is not in the TR, then $\bar{\gamma}$ can still be found simply by inspection; again it will either be equal to one or vary as $1/R^2$, and P_r will thus vary with either $1/R^2$ or $1/R^4$ behavior. But if the target is in the TR and there is jitter, then $\bar{\gamma}$ will have to be, in general, calculated from Eqs. (23) and (24).* The table below summarizes the four cases and their concomitant radar regions.

Case	Conditions	Radar Regions
I	$F \neq 1$ and jitter	$1/R^2$, TR (sometimes $1/R^3$), and $1/R^4$
II	$F \neq 1$ and negligible jitter	$1/R^2$, TR (always $1/R^3$), and $1/R^4$
III	$F = 1$ and jitter	$1/R^2$, TR and $1/R^4$
IV	$F = 1$ and negligible jitter	$1/R^2$ and $1/R^4$

For an arbitrary set of parameters yielding the four cases, the mean received power $\bar{P}_r$ has been plotted vs R for Cases I and II (Fig. 10a) and Cases III and IV (Fig. 10b) The parameters for all four cases are

$P_t = 8\,MW$ $\qquad$ $\beta = 0^\dagger$

$\sigma^0 = 1\ m^2/m^2$ $\qquad$ $\theta_x = \theta_z = 0.5$ mrad

$A_r = 10^{-2} m^2$ (4.4-in.-diam optics) $\qquad$ $\Delta_x = \Delta_z = 0.1$ mrad (Cases I and III only) .

*However, two unique situations may occur in which, even in the presence of jitter, $\bar{\gamma}$ can still be found by inspection, and again varies as $1/R$ (see App. F).

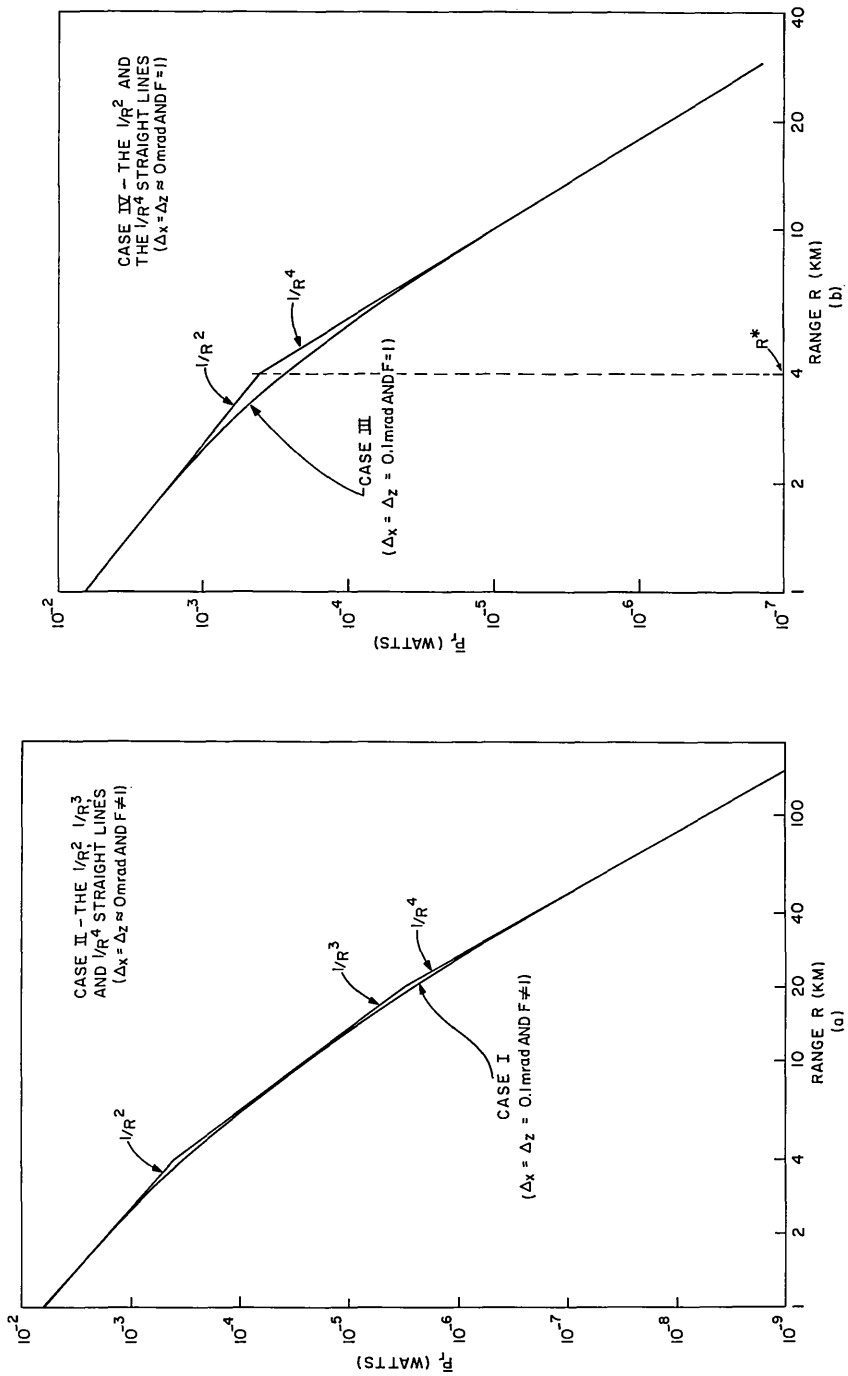

Fig. 10 – Mean received power $\bar{P}_r$ vs range R for (a) Cases I and II where $F \neq 1$ (in this instance $F = 1/5$) and $L_{Tz} = 10$ m, and (b) Cases III and IV where $F = 1$ and $L_{Tz} = 2$ m. For all cases $P_t = 8 \times 10^6$ W, $\sigma^0 = 1$ m²/m², $A_r = 10^{-2}$ m², $\beta = 0$, $\theta_x = \theta_z = 0.5$ mrad, $\Delta_x = \Delta_z = 0.1$ mrad (Cases I and III only), and $L_{Tx} = 2$ m.

Thus, $M = 6.37\times10^{-3}$ and $\bar{P}_r = 6.37\times10^{3}\ \bar{\gamma}/R^2$. In Fig. 10(a), $L_{Tx} = 2\text{m}$, $L_{Tz} = 10\text{m}$, and $F = (L_{Tx}/L_{Tz})/\theta_x/\theta_z = 1/5$. In Fig. 10(b), $L_{Tx} = L_{Tz} = 2\text{m}$, and $F = 1$.

The transition regions for the four cases are

Case I, $F \neq 1$ and Jitter $(k = k' = 5)$:

$$R_x = \frac{L_{Tx}}{\theta_x - 4\Delta_x} = \frac{2\ \text{m}}{0.5\ \text{mrad} - 0.4\ \text{mrad}} = 20\ \text{km}$$

and

$$R_z = \frac{L_{Tz}}{\theta_z - 4\Delta_z} = \frac{10\ \text{m}}{0.1\ \text{mrad}} = 100\ \text{km}\ ;$$

therefore the $1/R^4$ region starts at 100 km. Also,

$$R'_x = \frac{L_{Tx}}{\theta_x + 4\Delta_x} = \frac{2\ \text{m}}{0.9\ \text{mrad}} = 2.2\ \text{km}$$

and

$$R'_z = \frac{L_{Tz}}{\theta_z + 4\Delta_z} = \frac{10\ \text{m}}{0.9\ \text{mrad}} = 11.1\ \text{km}\ ;$$

therefore, the $1/R^2$ region starts at 2.2 km. Thus the TR extends from 2.2 km to 100 km.

Case II, $F \neq 1$ and $\Delta_x = \Delta_z = 0$ mrad:

$$R_x = R'_x = \frac{L_{Tx}}{\theta_x} = \frac{2\ \text{m}}{1/2\ \text{mrad}} = 4\ \text{km}$$

and

$$R_z = R'_z = \frac{L_{Tz}}{\theta_z} = \frac{10\ \text{m}}{1/2\ \text{mrad}} = 20\ \text{km}\ ;$$

therefore, the TR extends from 4 km to 20 km.

Case III, $F = 1$ and Jitter $(k = k' = 5)$:

$$R_x = R_z = \frac{L_{Tx}}{\theta_x - 4\Delta_x} = \frac{2\ \text{m}}{0.5\ \text{mrad} - 0.4\ \text{mrad}} = 20\ \text{km}$$

and

$$R'_x = R'_z = \frac{2\ \text{m}}{0.9\ \text{mrad}} = 2.2\ \text{km}\ ;$$

therefore, the TR extends from 2.2 km to 20 km.

Case IV, $F = 1$ and $\Delta_x = \Delta_z = 0$ mrad:

$$R_x = R'_x = R_z = R'_z = R^* \equiv \frac{L_{Tx}}{\theta_x} \equiv \frac{L_{Tz}}{\theta_z} = \frac{2\ \text{m}}{1/2\ \text{mrad}} = 4\ \text{km}\ .$$

Thus, for Case IV there is no TR, just a break point at R^* (4 km here) between the $1/R^2$ and the $1/R^4$ regions.

Even though Cases I and II appear to touch in Fig. 10(a) at about 10 km, they don't — the actual values of $\bar{P}_r$ at this range are

$$\text{Case I}, \quad \bar{P}_r = 2.47 \times 10^{-5} \text{ watts}$$

and

$$\text{Case II}, \quad \bar{P}_r = 2.55 \times 10^{-5} \text{ watts}.$$

In Cases I and III, if the jitter is neglected, then the error at any range can be found by examining the nonjitter cases, i.e., Cases II and IV, and then comparing either II to I or IV to III, depending on whether or not F equals one. The maximum differences (or errors) for the cases chosen will now be found. In Figs. 10(a) and 10(b) it is seen that the maximum errors occur where the straight lines cross.

In Fig. 10(a), where $F \neq 1$, at $R = 4$ km, Case II gives $\bar{P}_r = 4.0 \times 10^{-4}$ watts, Case I gives 3.4×10^{-4} watts, the ratio II/I = 1.18, and Case II is 18% too high. At $R = 20$ km, Case II gives 3.2×10^{-6} watts, Case I gives 2.7×10^{-6} watts, the ratio II/I = 1.19, and Case II is 19% too high. In Fig. 10(b), where $F = 1$, at $R = 4$ km, Case IV gives $\bar{P}_r = 4.0 \times 10^{-4}$ watts, Case III gives 2.8×10^{-4} watts, the ratio IV/III = 1.43, and Case IV is 43% too high.

When $F = 1$ (in Fig. 10(b)), it is seen that maximum difference or error between Cases IV and III occurs at the Case IV breakpoint range, R^*, where the $1/R^2$ and $1/R^4$ lines cross. An equation for determining this percentage difference at R^*, without having to calculate $\bar{P}_r$ for Cases III and IV, will now be derived.*

In regard to Case IV, $\bar{\gamma}_x = \bar{\gamma}_z = 1$ at R^*, and thus at R^*, $\bar{\gamma}$ is 1.

In regard to Case III, equations must now be found for $\bar{\gamma}_x$ and $\bar{\gamma}_z$ at the range R^* in order to find $\bar{\gamma}$ at this range. At $R = R^*$, the equality $L_{Bx} = L_{Tx}$ holds since $L_{Bx} = \theta_x R$ and $R^* = L_{Tx}/\theta_x$. Therefore $y_1 = 0$ and $y_2 = L_{Bx}/\Delta_x' = k$, and thus Eq. (23) becomes

$$\bar{\gamma}_x = \frac{2}{L_{Bx}} (G_2 L_{Bx} + \Delta_x' E_1) ,$$

where

$$G_2 = \int_0^k \phi(y)\, dy ,$$

and

$$E_1 = \phi(y)\Big|_0^k = e^{-y^2/2}\Big|_0^k \Big/ \sqrt{2\pi} = 0.4\, e^{-y^2/2}\Big|_0^k .$$

If $k \geq 4$, then $G_2 \approx 1/2$ and $E_1 \approx -0.4$. Therefore, $\bar{\gamma}_x = 1 - (0.8/k) = a$† if $k \geq 4$; similarly in the z direction if $k' \geq 4$, then $\bar{\gamma}_z = 1 - (0.8/k') = b$; and thus at $R = R^*$, $\bar{\gamma} = ab$ if $k \geq 4$ and $k' \geq 4$.

*When $F \neq 1$, a similar derivation of a simple equation doesn't appear feasible.
†Equation (24) will give the same result.

Thus, at R^*, where the maximum difference occurs between the mean received power $\bar{P}_r$ for Cases IV and III, the maximum difference in $\bar{\gamma}$ also occurs, and this difference on a percentage basis is equal to $[(1 - ab)/ab] \times 100$. Thus, the percentage difference (PD) is

$$PD = \frac{1 - (1 - 0.8/k)(1 - 0.8/k')}{(1 - 0.8/k)(1 - 0.8/k')} . \tag{39}$$

If $k = k'$, then Eq. (39) reduces to

$$PD = \frac{1.6(k - 0.4)}{(k - 0.8)^2} . \tag{40}$$

As a check to the previous error calculation of 43% comparing Case IV to Case III, $k = 5$ is inserted into Eq. (40). The result, 42%, is reasonably close.

CONCLUSION

Via the introduction of a new parameter, $\bar{\gamma}$, a generalized laser radar range equation has been derived which is valid at any range for a flat target of any size and shape and with any type of reflective properties; in addition, this equation is valid no matter what shape the laser beam has, nor its degree of divergence and jitter.

When, with regard to the range equation, the received power $\bar{P}_r$ varies with neither a $1/R^2$ nor a $1/R^4$ dependency, then the target is said to be in a transition region (TR) between the $1/R^2$ region and the $1/R^4$ region. From an inspection of the equations for $\bar{\gamma}$, the boundary equations of the TR have been found. In addition, the parametric behavior of the TR has been analyzed with regard to its causative agents — spatial jitter and the degree of shape mismatching between the beam and the target.

Two basic types of situations occur: one when the jitter is negligible, the other when the jitter isn't negligible.

When jitter is negligible, $\bar{\gamma}$ can be found by inspection in all three regions. In the TR, $\bar{P}_r \propto 1/R^3$, and thus, $\bar{P}_r \propto 1/R^2$, $1/R^3$, and $1/R^4$ in the three regions. As the degree of shape mismatching between the beam and target is reduced, the TR shrinks until, when there is no mismatch, there is no TR; then just the $1/R^2$ and $1/R^4$ regions remain.

If the jitter is not negligible, $\bar{\gamma}$ can still be found by inspection in the $1/R^2$ and $1/R^4$ regions, but it must, in general, be calculated when the target is in the TR. Because of jitter, a TR will always exist whether or not there is any shape mismatching.

Errors in $\bar{P}_r$ caused by neglecting jitter can be found by comparing the $\bar{P}_r$ vs R curves with and without jitter. The maximum errors occur at the zero-jitter breakpoints and these can easily be found. Typical errors can be as much as 40% or more.

In regard to errors, the neglecting of significant jitter shouldn't cause the basic results of the system designer to be invalid, and the "three (or two) straight lines" approximation should be adequate; however for the experimentalist trying to measure σ, the neglecting of significant jitter may lead to unacceptably large errors.

ACKNOWLEDGMENT

The author wishes to thank R. D. Tompkins for many helpful suggestions.

REFERENCES

1. Wyman, P.W., "Analysis of the Problem of Pointing a Laser Radar," NRL Report 6281, Oct. 7, 1965

2. Nicodemus, F.E., in "Applied Optics and Optical Engineering," Vol. 4, Chap. 8, R. Kingslake, ed., New York:Academic Press, 1967

3. "Handbook of Military Infrared Technology," W.L. Wolfe, ed., Chap. 2, W.L. Wolfe and F.E. Nicodemus, Office of Naval Research, Wash., D.C.:U.S. Government Printing Office, 1965

4. Nicodemus, F.E., "Emissivity of Isothermal Spherical Cavity with Gray Lambertian Walls," Appl. Opt. 7:1359 (July 1968)

5. Ridenour, L.N., ed., "Radar System Engineering," p. 21, New York:McGraw-Hill, 1947

6. Wyman, P.W., "Definition of Laser Radar Cross Section," Appl. Opt. 7:207 (Jan. 1968)

7. "Propagation of Short Radio Waves," D.E. Kerr, ed., p. 483, New York:McGraw-Hill, 1951

Appendix A

COMMENTS ON THE $1/R^4$ RANGE EQUATION

When $R \geq R_x$ or R_z, depending on which is larger,

$$\bar{\gamma} = \frac{L_{Tx}L_{Tz}}{L_{Bx}L_{Bz}} = \frac{L_{Tx}L_{Tz}}{A_B} = \frac{L_{Tx}L_{Tz}}{\Omega_t R^2} = A_i/A_B \ .$$

(See section regarding $1/R^4$ region, beginning on p. 7.) Substituting into Eq. (20) yields

$$\bar{P}_r = (P_t/\Omega_t)\tau^2\sigma^0 L_{Tx}L_{Tz}A_r/4\pi R^4 \ . \tag{A1}$$

Since now $A_i = L_{Tx}L_{Tz}$ and $\sigma = \sigma^0 A_i$ (Eq. (18)), $\sigma = \sigma^0 L_{Tx}L_{Tz}$. Using this relationship and the gain definitions of the transmitter $(G_t = 4\pi/\Omega_t)$ and the receiver $(G_r = 4\pi A_r/\lambda^2)$ yields

$$\bar{P}_r = P_t G_t G_r \tau^2 \lambda^2 \sigma/(4\pi)^3 R^4 \tag{A2}$$

which is one of the more familiar (5) forms of the radar range equation.

As a point of interest, if the target is normal to the beam

$$w_T h_T = A_T = L_{Tx}L_{Tz} = A_i \ ,$$

and therefore

$$\sigma = \sigma^0 A_T \ . \tag{A3}$$

Thus, it is seen that this commonly stated relationship only holds for a target normal to the beam and in the $1/R^4$ region, and is otherwise not valid.

Appendix B

COMMENTS ON THE $1/R^2$ RANGE EQUATION

When $R \leq R'_x$ or R'_z, depending on which is smaller, $\bar{\gamma} = 1$. (See section regarding $1/R^2$ region, beginning on p. 9.) Substituting into Eq. (20) yields

$$\bar{P}_r = P_t \tau^2 \sigma^0 A_r / \left(4\pi R^2\right). \tag{B1}$$

In Eq. (B1), we see that neither the area nor the aspect of the target influences the received power $\bar{P}_r$. The solid angle of the transmitter also does not effect $\bar{P}_r$.

Jelalian* has recently used a pulsed Nd laser radar to indirectly measure the σ^0 of the ocean (in various sea states) and of sand. The laser was airborne and pointed straight down over the target of interest and $\bar{P}_r$ was measured. P_t, A_r, and R were known and τ was estimated, and thus σ^0 was calculated using Eq. (B1).

*A.V. Jelalian, "Sea Echo at Laser Wavelengths," Proc. IEEE 56:828 (May 1968).

Appendix C

RANGE EQUATIONS WHEN THE RECEIVED BEAM IS SMALLER THAN THE RECEIVER

When a target is highly specular (or if it is retroreflective), there is the likelihood that the reflected beam, at the receiver, will be smaller than the receiver. This is shown in Fig. C1. When this situation occurs, the mean received power is

$$\bar{P}_r = \tau \bar{P}_{ref} \tag{C1}$$

and the mean reflected power is

$$\bar{P}_{ref} = \tau P_t \bar{\gamma} \rho_d \tag{C2}$$

where ρ_d is the bidirectional reflectance (it will be discussed more in Appendix D). Therefore,

$$\bar{P}_r = \tau^2 \rho_d P_t \bar{\gamma} \ . \tag{C3}$$

This is the general range equation for this situation. Now let us look at two special cases:

(a) When $R \geq R_x$ or R_z, depending on which is greater, $\bar{\gamma} \approx L_{Tx} L_{Tz} / \Omega_t R^2 = A_i / A_B$, and when this occurs

$$\bar{P}_r \approx \tau^2 \rho_d J_t L_{Tx} L_{Tz} / R^2 \tag{C4}$$

This could be referred to as the "small target" case. If the system is almost lossless, i.e., if $\tau \approx 1$ and $\rho_d \approx 1$, then since $L_{Tx} L_{Tz} = A_i$, the mean received power is

$$\bar{P}_r \approx J_t (A_i / R^2) \ . \tag{C5}$$

Since A_i / R^2 equals the target solid angle (at the transmitter), the received power is approximately equal to the power hitting the target.

(b) When $R \leq R'_x$ or R'_z, depending on which is less, $\bar{\gamma} \approx 1$ and when this occurs

$$\bar{P}_r \approx \tau^2 \rho_d P_t \ . \tag{C6}$$

This could be referred to as the "extended target" case. If $\tau \approx 1$ and $\rho_d \approx 1$, the received power is approximately equal to the transmitted power.

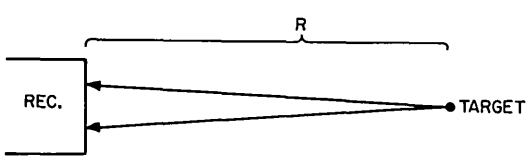

Fig. C1 - Geometry for the special case where the received beam is smaller than the receiver

Appendix D

REFLECTIVE PROPERTIES OF A SURFACE

In the derivation of the laser radar range equation the following parameters describing a surface were introduced — the bidirectional reflectance-distribution function ρ', and the target cross section per unit area σ^0. It was shown that they are related to each other by $\sigma^0 = 4\pi\rho'$ when ρ' and the incident irradiance H_i are constant over the target* and ρ' is independent of H_i. In Appendix C the bidirectional reflectance ρ_d was introduced, and now the questions arise as to how ρ_d and ρ' are related to each other and how these two parameters are related to ρ, the overall reflectance of a surface.

In Refs. 2 and 3, ρ_d is defined as

$$\rho_d \text{ (dimensionless)} = \int_{\text{hemisphere}} \rho' \, d\Omega_r' \tag{D1}$$

where $d\Omega_r' = \sin\psi_r \cos\psi_r \, d\psi_r \, d\alpha_r$, and ψ_r and α_r are the elevation and azimuth angles of reflection, respectively. Therefore,

$$\rho_d = \int_h \rho' \sin\psi_r \cos\psi_r \, d\psi_r \, d\alpha_r \, .$$

For most surfaces ρ' is not dependent on α_r, and therefore

$$\rho_d = 2\pi \int_0^{\pi/2} \rho' \sin\psi_r \cos\psi_r \, d\psi_r \tag{D2}$$

since

$$\int_0^{2\pi} d\alpha_r = 2\pi \, .$$

For a perfectly diffuse surface, ρ' is dependent on neither α_r nor ψ_r, and therefore

$$\rho_d = 2\pi\rho' \int_0^{\pi/2} \sin\psi_r \cos\psi_r \, d\psi_r = \pi\rho' \tag{D3}$$

or

$$\rho' = \rho_d/\pi \; (sr^{-1}) \tag{D4}$$

---

*ρ' and σ^0 are both measured along the radar line of sight.

For a perfectly specular surface at the proper viewing angle (2), $N_r = \rho_d N_i$, and this yields $P_r = \rho_d P_i$ which was the basis of Eq. (C2).

The other parameter of interest here is the reflectance ρ of a surface. It is defined in Refs. 2 and 3 as

$$\rho = \partial P_r / \partial P_i \tag{D5}$$

According to the terminology of the National Bureau of Standards* this parameter more completely should be called the bihemispherical reflectance $\rho(2\pi:2\pi)$, since ρ is the ratio between the power reflected in all directions and the power incident from all directions. Judd's reference also discusses in great detail the many other types of reflectance and the interrelationships between them. From either this reference or from Ref. 3, the following relationship is found:

$$\rho = \frac{1}{\pi} \int_h \rho_d \, d\Omega_r' \ . \tag{D6}$$

If ρ_d is not a function of α_r, then

$$\rho = 2 \int_0^{\pi/2} \rho_d \sin\psi_r \cos\psi_r \, d\psi_r \tag{D7}$$

For a diffuse surface, $\rho_d = \pi\rho'$ and ρ' is independent of both α_r and ψ_r. Therefore,

$$\rho = 2\pi\rho' \int_0^{\pi/2} \sin\psi_r \cos\psi_r \, d\psi_r \ ,$$

and therefore,

$$\rho = \pi\rho' = \rho_d \ . \tag{D8}$$

Finally, for a diffuse surface $\sigma^0 = 4\pi\rho' = 4\rho_d = 4\rho$. The reason for the appearance of the 4 is because σ is defined here relative to an isotropic target, not to a diffuse flat plate as is sometimes done.

Occasionally (see footnote reference to Jelalian in Appendix B) a parameter is introduced which in a way describes the reflective properties of a surface. It is called the effective solid angle of return Ω. It is defined as

$$\Omega \equiv \rho_d / \rho' \tag{D9}$$

Therefore,

$$\Omega = \frac{\int_h \rho' \, d\Omega_r'}{\rho'} \ . \tag{D10}$$

For a diffuse surface ρ' is independent of both ψ_r and α_r, and therefore

*D.B. Judd, "Terms, Definitions, and Symbols in Reflectometry," J. Opt. Soc. Am. 57:445 (April 1967).

$$\Omega = \int_h d\Omega_r' = 2\pi \int_0^{\pi/2} \sin\psi_r \cos\psi_r \, d\psi_r$$

or $\Omega = \pi$ for a diffuse surface. Combining Eqs. (D4) and (D9) will give the same result.

Substituting Eq. (D9) into Eq. (19) yields

$$\sigma^0 = 4\pi \rho_d/\Omega . \tag{D11}$$

This is Eq. 4 in Jelalian's paper. It is seen that σ^0 increases as either ρ_d increases or as Ω decreases. Specular and retroreflective surfaces can sometimes have very small Ω's, and consequently large σ^0's and σ's.

The degree of diffuseness is the degree to which ρ' is constant versus ψ_r, and this depends on the relative surface roughness or granularity at the wavelength of interest. In the optical region a heavy layer of dust can change a highly specular surface to one that is highly diffuse. However, when a standard diffuse surface is needed, special materials must be used. Saiedy and Jones* present measurements on ρ' vs ψ_r for the following materials: vitrolite, ceramic felt (Fiberfrax from the Carborundum Co.), artificial quartz, smoked M_gO, pressed M_gO, and 3M white paint (Type 401-A-10). Tytten and Flowers† present earlier measurements, but for fewer materials. Grum and Luckey‡ present measurements on barium sulfate coatings which appear to be very good in the 0.20-2.0 μm region.

*F. Saiedy and G.D. Jones, "Bidirection Reflectance Measurements for Satellite Calibration Target in the Visible and Near Infrared," Appl. Opt. 7:429 (March 1968).

†G. Trytten and W. Flowers, "Optical Characteristics of a Proposed Reflectance Standard," Appl. Opt. 5:1895 (Dec. 1966).

‡F. Grum and G.W. Luckey, "Optical Sphere Paint and a Working Standard of Reflectance," Appl. Opt. 7:2289 (Nov. 1968).

Appendix E

ONE-WAY ATMOSPHERIC TRANSMISSION LOSS τ

INTRODUCTION

Atmospheric attenuation is due to three effects: Mie or particle scattering, Rayleigh or molecular scattering, and absorption.* Associated with each effect is an attenuation coefficient, β_p, β_m, and β_a, respectively, which may depend on the propagation path distance R (see Fig. E1). These coefficients are additive† so that the overall attenuation coefficient β is

$$\beta = \beta_p + \beta_m + \beta_a \ . \tag{E1}$$

The basic relationship between the intensity J and β is†

$$dJ/J = -\beta(R)\ dR \ . \tag{E2}$$

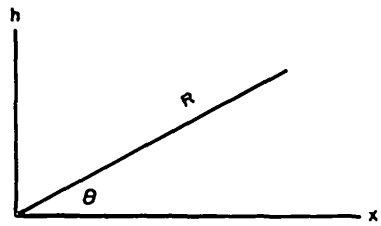

Fig. E1 - Propagation path geometry

In the visible region β_a is negligible, and therefore

$$\ln J = -\int(\beta_p + \beta_m)\ dR \ . \tag{E3}$$

Table E1 (from Campen) gives the values of β_p and β_m at various altitudes at a wavelength of 0.55 μm. An examination of this table shows that both parameters decrease approximately exponentially with the altitude h, i.e.,

$$\beta_p(h) = \beta_p(0)\ e^{-k_2 h} = k_1\ e^{-k_2 h} \tag{E4}$$

and

$$\beta_m(h) = \beta_m(0)\ e^{-k_4 h} = k_3\ e^{-k_4 h} \ . \tag{E5}$$

*C.F. Campen, et al., eds., "Air Force Handbook of Geophysics," p. 14-13, New York: Macmillan, 1960.
†F.A. Jenkins and H.E. White, "Fundamentals of Optics," pp. 200, 447, and 461, 3rd ed., New York: McGraw-Hill, 1957.

Table E1
Molecular and Particle Scattering Coefficients vs Height in Uniform Atmosphere with Ground Visibility of 10 Nautical Miles

Height h (kilofeet)	$\beta_m(h)$ (naut mi)$^{-1}$	$\beta_p(h)$ (naut mi)$^{-1}$
0	0.0234	0.3678
10	0.0160	0.0290
20	0.0109	0.0023
30	0.0075	0.0001
40	0.0051	0.00005
50	0.0035	< 0.00005
60	0.0023	< 0.00005
70	0.0016	< 0.00005
80	0.0011	< 0.00005
90	0.0008	< 0.00005
100	0.0005	< 0.00005

The constants are as follows:

$k_1 = \beta_p(0)$ = particle scattering coefficient at ground level ($h = 0$),

k_2 = inverse of the particle scattering scale height = 0.83 km^{-1},*

$k_3 = \beta_m(0)$ = molecular scattering coefficient at ground level, and

k_4 = inverse of the molecular scattering scale height = 0.13 km^{-1}.*

For the values listed in Table E1 (where the visibility = 10 naut mi),

k_1 = 0.368 (naut mi)$^{-1}$ = 0.199 km^{-1},

k_3 = 0.023 (naut mi)$^{-1}$ = 0.0124 km^{-1}, and

$\beta(0) = k_1 + k_3$ = 0.391 (naut mi)$^{-1}$ = 0.211 km^{-1}.

OVER A HORIZONTAL PATH

Along a horizontal path ($R = x$) β is fairly constant with distance, and therefore

$$\ln J = -\beta \int dx = -\beta x + C ,$$

which yields

$$\tau = J/J_0 = e^{-\beta x} \tag{E6}$$

where J_0 is the intensity at $x = 0$ and the ratio J/J_0 is defined as τ, the one-way atmospheric transmission loss. The horizontal visibility or meteorological range V (see footnote to Campen reference) is that range at which τ at 0.55 μm equals 0.02. Therefore,

*1.852 km = 1 naut mi.

$$\tau = 0.02 = e^{-\beta V} = e^{-3.91} , \tag{E7}$$

from which

$$V = 3.91/\beta_{0.55\ \mu m} . \tag{E8}$$

As a check, the $\beta(0)$ from Table E1 can be inserted into Eq. (E8), which yields

$$V = 3.91/0.391 = 10 \text{ naut mi.}$$

OVER A VERTICAL PATH

For a vertical propagation path, the distance R is equal to h. If absorption can be ignored, then Eq. (E3) can be written as

$$\ln J = - \int (\beta_p + \beta_m)\, dh .$$

Substituting Eqs. (E4) and (E5) yields

$$\ln J = - \int \left(k_1\ e^{-k_2 h} + k_3\ e^{-k_4 h} \right) dh . \tag{E9}$$

Equation (E9) yields

$$\tau = \exp\left[-\left(k_1/k_2\right)\left(1 - e^{-k_2 h}\right) - \left(k_3/k_4\right)\left(1 - e^{-k_4 h}\right) \right] . \tag{E10}$$

At $h = 0$, $\tau = 1$, and at $h = \infty$, $\tau = e^{-k''}$ where $k'' \equiv (k_1/k_2) + (k_3/k_4)$.

Figure E2 is a plot of Eq. (E10) when $k'' = 0.34$. The value $k'' = 0.34$ comes from the previously used values of k_1, k_2, k_3, and k_4 when $V = 10$ naut mi. Using this value for k'' yields

$$e^{-k''} = e^{-0.34} \approx 0.71 .$$

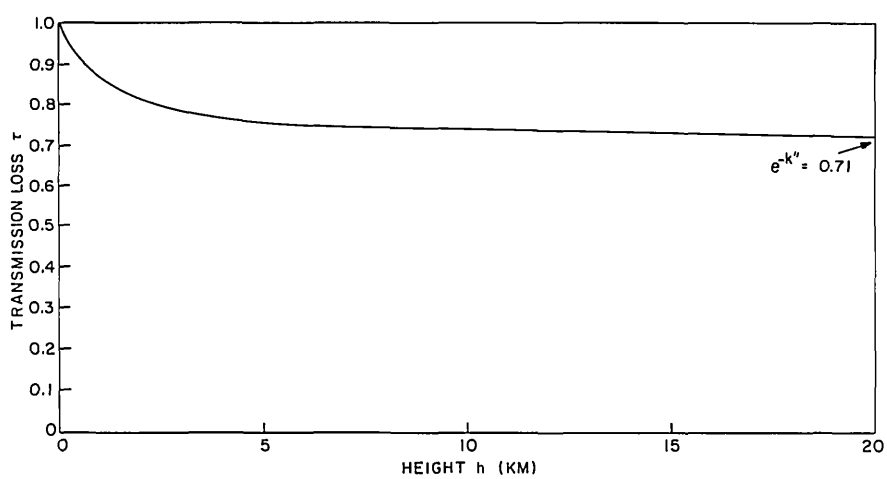

Fig. E2 - One-way transmission loss τ vs height h for a vertical propagation path when $k'' = 0.34$

Therefore, the minimum vertical transmission $(\tau_h)_{min}$ equals 0.71. If this minimum τ_h is equated with a τ_x over some given distance along the ground, then $\tau_x = (\tau_h)_{min}$, and therefore $e^{-\beta(0)x} = e^{-k''}$, which yields

$$x = k''/\beta(0) = 0.34/0.211 \text{ km}^{-1} = 1.6 \text{ km } (0.87 \text{ naut mi}) .$$

Thus, at 0.55 μm when the ground visibility is 10 naut mi, the attenuation over about a 1-naut-mile horizontal path is equal to the attenuation along a vertical path through all of the atmosphere.

OVER A SLANT PATH

For slant path propagation, $h = R \sin\theta$, and therefore Eqs. (E4) and (E5) become

$$\beta_p(R) = k_1 \, e^{-k_2 R \sin\theta}$$

and

$$\beta_m(R) = k_3 \, e^{-k_4 R \sin\theta} .$$

Letting $k_2' = k_2 \sin\theta$ and $k_4' = k_4 \sin\theta$ and using $\ln J = -\int \beta(R)\, dR$, results in

$$\ln J = -\int \left(k_1 \, e^{-k_2' R} + k_3 \, e^{-k_4' R} \right) dR$$

since $\beta(R) = \beta_p(R) + \beta_m(R)$. Therefore,

$$\tau = J/J_0 = \exp\left[-\left(k_1/k_2'\right)\left(1 - e^{-k_2' R}\right) - \left(k_3/k_4'\right)\left(1 - e^{-k_4' R}\right) \right] \tag{E11}$$

or

$$\tau = \exp\left[-\left(k_1/k_2'\right)\left(1 - e^{-k_2 h}\right) - \left(k_3/k_4'\right)\left(1 - e^{-k_4 h}\right) \right] . \tag{E12}$$

Appendix F

SPECIAL SECTION OF THE TRANSITION REGION WHEN $F \neq 1$

When F doesn't equal one, a transition region (TR) always exists. In this TR, when the jitter is negligible, it has been shown that $\bar{\gamma}$ can be found by inspection and that it varies as $1/R$, with the result that $\bar{P}_r \propto 1/R^3$ (see section beginning on p. 13). However, it was also stated there that when $F \neq 1$, "if the target is in the TR and there is jitter, then $\bar{\gamma}$ will have to be, in general, calculated from Eqs. (23) and (24)."

The reason for adding the phrase "in general" is because under certain circumstances $\bar{\gamma}$ can still be found by inspection under these conditions. The following two situations prove this statement.

a. If $R_z' \geq R \geq R_x$, then $R \leq R_z'$ yields $\bar{\gamma}_z = 1$, and $R \geq R_x$ yields $\bar{\gamma}_x = (L_{Tx}/\theta_x)/R$. Therefore, under this situation (the target between R_z' and R_x when $R_z' \geq R_x$),

$$\bar{\gamma} = \frac{(L_{Tx}/\theta_x)}{R} \quad \text{and} \quad \bar{P}_r \propto 1/R^3 \ .$$

b. If $R_x' \geq R \geq R_z$, then $R \leq R_x'$ yields $\bar{\gamma}_x = 1$, and $R \geq R_z$ yields $\bar{\gamma}_z = (L_{Tz}/\theta_z)/R$. Therefore, under this situation (the target between R_x' and R_z when $R_x' \geq R_z$),

$$\bar{\gamma} = \frac{(L_{Tz}/\theta_z)}{R} \quad \text{and} \quad \bar{P}_r \propto 1/R^3 \ .$$

In the general example shown in Fig. 9 the first situation existed because $R_z' = 3.33$ km and $R_x = 1.67$ km; but in Fig. 10(a), even though the "with jitter" line appears to touch the $1/R^3$ line, it was shown that it doesn't. This latter result is confirmed by noting that neither of the above two situations is met, and thus the $1/R^3$ approximation is still slightly in error even at a range of about 10 km.

Security Classification

DOCUMENT CONTROL DATA - R & D

(Security classification of title, body of abstract and indexing annotation must be entered when the overall report is classified)

1. ORIGINATING ACTIVITY *(Corporate author)* Naval Research Laboratory Washington, D.C. 20390	2a. REPORT SECURITY CLASSIFICATION Unclassified 2b. GROUP

3. REPORT TITLE

LASER RADAR RANGE EQUATION CONSIDERATIONS

4. DESCRIPTIVE NOTES *(Type of report and inclusive dates)*
A final report on one phase of the problem.

5. AUTHOR(S) *(First name, middle initial, last name)*

P.W. Wyman

6. REPORT DATE December 11, 1969	7a. TOTAL NO. OF PAGES 36	7b. NO. OF REFS 7
8a. CONTRACT OR GRANT NO. NRL Problems R02-24A, R05-29, and R06-38 b. PROJECT NO. AO-535-208/652-1/F099-05-02 and c. RF-17-344-401-4509 d. SS33-18-11917	9a. ORIGINATOR'S REPORT NUMBER(S) NRL Report 6971 9b. OTHER REPORT NO(S) *(Any other numbers that may be assigned this report)*	

10. DISTRIBUTION STATEMENT

This document has been approved for public release and sale; its distribution is unlimited.

11. SUPPLEMENTARY NOTES	12. SPONSORING MILITARY ACTIVITY Department of the Navy (Naval Air Systems Command, Office of Naval Research, and Naval Ship Engineering Center), Washington, D.C.

13. ABSTRACT

Starting with basic physical and beam-target-geometry concepts, a generalized laser radar range equation is derived which holds for a target at any range R in the far field. The equation takes the form $\bar{P}_r \propto \bar{\gamma}/R^2$, where $\bar{P}_r$ is the mean value of the received power and $\bar{\gamma}$ is the mean value of the fraction of the laser beam hitting the target.

By examining the equations for $\bar{\gamma}$, other equations are found for the boundaries of the three radar regions — the $1/R^2$ region, the transition region, and the $1/R^4$ region. These boundaries, and $\bar{\gamma}$ itself, are functions of the spatial jitter of the beam and the degree to which the shape of the beam and the shape of the target geometry are not the same. In the transition region when the jitter is negligible, $\bar{\gamma}$ can be found by inspection (as can be done in the $1/R^2$ and $1/R^4$ regions whether or not the jitter is negligible); the resultant received power then varies as $1/R^3$. In the transition region when the jitter is not negligible, $\bar{\gamma}$ must be calculated from equations before $\bar{P}_r$ can be calculated. For completeness, the reflective properties of a target, its cross section, and the one-way atmospheric transmission loss are examined. The relationships derived in this report are general in that they are valid at any (e.g., microwave) wavelengths.

DD FORM 1 NOV 65 1473 (PAGE 1)

S/N 0101-807-6801

Security Classification

14. KEY WORDS	LINK A		LINK B		LINK C	
	ROLE	WT	ROLE	WT	ROLE	WT
Laser beams						
Optical radar						
Range (distance)						

DD FORM 1 NOV 65 1473 (BACK)
(PAGE 2)